Differential cross sections for symmetrical ion-atom collisions in the rare gases.

A. V. Phelps

JILA, University of Colorado and National Institute of Standards and Technology, Boulder, Colorado 80309-0440

(Dated: November 27, 2007)

Abstract

Approximate differential cross sections for elastic collisions of rare gas ions with their parent atoms are proposed for He^+-He, Ne^+-Ne, Ar^+-Ar, Kr^+-Kr, and Xe^+-Xe collisions for collision energies from ~ 0.1 eV to 10 keV. The basic assumption of the generic model is that the scattering of the ion by the atom is determined by the interaction potential that would be present in the absence of symmetry considerations. This potential is assumed to be dominated by the polarization interaction. We further assume that the scattering can be described classically and that charge transfer effects lead to reflection about 90°. Corrections are made for forward diffraction and the absence of charge transfer effects in the near backward direction. The empirical differential cross sections are compared with the few available results from quantum mechanical theory and scattering experiments. Our results are formulated in terms of analytical expressions for use in models of discharge plasmas, etc.

See files SYMMCOLL.TEX, SYMMCOL.PDF, and SymmIonAtomCollision.pdf.

PACS numbers: PACS numbers: 34.50.-s; 34.20.-b; 52.20.Hv

I. INTRODUCTION

We propose a scalable classical formula based on polarization scattering for use in estimating the elastic differential cross section for collisions between rare gas ions and their parent atoms, e.g., those of Ar+ with Ar. Our motivations for this study include continued requests for these differential cross sections for discharge modelling and the extreme shortage of either experimental or theoretical differential cross sections. We expect that these ideas will apply to other ion-parent atom collisions.

What we do here is a lot like what was done by Nanbu and Kitatani [1]. They did a Monte Carlo calculation of ion transport using classical scattering with a polarization potential having a hard sphere radius determined by fitting to mobility data at high E/n where charge transfer dominates. They found it necessary to apply a small angle (large impact parameter) cutoff in their scattering model so as to obtain a finite total cross section as required by their Monte Carlo calculations.

II. CLASSICAL CROSS SECTIONS

From McDaniel, Mitchell, and Rudd [2] the classical differential scattering cross section in a.u. for a polarization potential in atomic units of $V(r) = -cr^{-4}$ at small angles is given by:

$$I_{sm}(\theta) = ((3\pi)^{1/2}/8)(c/(E_{relau}\theta))^{1/2}/(\theta \sin[\theta]) \tag{1}$$

Here θ is the scattering angle and E_{rel} is the relative collision energy, both in center-of-mass.

A more accurate approximation to the classical scattering for a polarization potential is obtained by numerically integrating Eq. (3-4-5) of McDaniel et al [2] for various impact parameters, eliminating the impact parameter variable, and fitting by trial and error to obtain

$$I_{cl}(\theta) = (0.07182 + 0.2713/\theta^{5/2} + 0.08637/\theta^{3/2})(\alpha_{au}/E_{relau})^{1/2} \tag{2}$$

Both $I_{sm}(\theta)$ and $I_{cl}(\theta)$ have $(\theta)^{-5/2}$ singularities at $\theta = 0$ and so cannot be integrated to give an integral or "total" scattering cross section [3]. $I_{sm}(\theta)$ has a stronger singularity at $\theta = \pi$ that prevents it being integrated to give a diffusion (momentum transfer) cross section [3].

My idea is to reflect the classical differential cross section about $\theta = \pi/2$ in center of mass. When doing so each part of the classical differential cross section given above must be divided by 2 to give the same viscosity cross section [3].

$$I_{ct}(\theta) = ((0.07182 + 0.2713/\theta^{5/2} + 0.08637/\theta^{3/2}) \tag{3}$$
$$+(0.07182 + 0.2713/(\pi - \theta)^{5/2} + 0.08637/(\pi - \theta)^{3/2})) * (\alpha_{au}/E^{(}_{relau}1/2)/2$$

This function has non-integrable $(\theta)^{-5/2}$ singularities at both $\theta = 0$ and π. The next section describes how we modify the assumed differential cross section so as to take into account these singularities.

III. TOTAL CROSS SECTION CORRECTION

IV. CHARGE TRANSFER CORRECTION

In order to follow this section it is critical that the reader accept the idea that symmetric charge transfer is just one aspect of elastic scattering [5]. This means that if one treats elastic scattering properly, then symmetric charge transfer has been properly accounted for in the collision process.

Our basic approach to charge transfer is to treat the elastic scattering classically, i.e., we assume that charge transfer only occurs within a certain impact parameter with its corresponding distance of closest approach. One possibility would be to set the distance of closest approach equal to distance at which the probability of charge transfer during a collision, as defined by Holstein [6] Instead, we have used a much more empirical approach in which the effective angular limit for charge transfer is set by the requirement that the diffusion cross section calculated using the modified classical cross section be equal to the diffusion cross section that we have determined from mobility experiments at low energies and from twice the charge transfer cross section given by beam experiments at high energies [4]. One advantage of our approach is that the ambiguities regarding the definition of symmetric charge transfer cross section at low energies are avoided [7].

TO DO - Discuss the integrated cross sections derived from this approximation with consideration of whether a) this is a useful technique for predicting charge transfer cross sections, b) the backward hemisphere is a good (more universal) definition of charge transfer

(see appendix for some of this), c) the possible correlation of charge transfer cross sections with polarization (usually the correlation is with ionization potential). Point out that our simplified classical model omits structure found in detailed classical and quantum models such as the peak scattering at the rainbow angle.

V. $H^+ + H$

Figures 1 through 4 show elastic differential cross sections versus scattering angle in center-of-mass for H^+ by H at 0.1, 1, 10 and 100 eV relative energy.

The solid curves are from Kristic and Schulz. [12] We note absence of a backward peak as expected for "classical" symmetric charge transfer. The orange curve a constant differential cross section on this type of plot.

The polarization curve without taking symmetric charge transfer into account. The purple curve is our construction based on reflection of the polarization scattering about 90°. The blue curve is our polarization curve modified for the finite range of symmetric charge transfer.

Elastic differential cross section (a_0^2/sr) versus scattering angle (°) in center-of-mass for H^+ by H at 1 eV relative energy. The solid curves are from Kristic and Schulz. [12] Note absence of a backward peak. The almost hidden purple curve is our construction based on reflection of the polarization scattering. The blue curve is our polarization curve modified for the finite range of symmetric charge transfer.

Figure 3 shows elastic differential cross section (a_0^2/sr) versus scattering angle (°) in center-of-mass for H^+ by H at 10 eV relative energy. The solid curves are from Kristic and Schulz. [12] The almost hidden purple curve is our construction based on reflection of the polarization scattering. The blue curve is our polarization curve modified for the finite range of symmetric charge transfer.

Figure 4 shows elastic differential cross section (a_0^2/sr) versus scattering angle in center-of-mass (°) for H^+ by H at 100 eV relative energy. The solid curves are from Kristic and Schulz. [12] The almost hidden purple curve is our construction based on reflection of the polarization scattering. The blue curve is our polarization curve modified for the finite range of symmetric charge transfer.

VI. $HE^+ + HE$

Figures 5 and 6 show elastic differential cross section versus scattering angle in center-of-mass for He^+ by He at 0.05 and 15 eV relative energy. The cyan curve are from Kristic and Schulz. [12] The purple curve is our construction from polarization scattering assuming symmetrical charge transfer means reflection about 90°. The red curve is our modification that roughly accounts for the finite range of symmetric charge transfer. Note absence of a backward peak in Fig. 5.

Figure **??** shows the elastic differential cross section versus scattering angle in center-of-mass for He^+ by He at 15 eV relative energy. The solid curves are from Kristic and Schulz. [12] The blue curve is our polarization curve reflected about 90° and modified for the finite range of symmetric charge transfer. The cyan points are from Vestal, Blakely, and Futrell [11].

VII. $NE^+ + NE$

VIII. $AR^+ + AR$

Figures 7 and 8 show elastic differential cross sections versus scattering angle in center-of-mass for Ar^+ by Ar at 2.76 and 10 eV relative energy. Note the reduction in the backward peak relative to the forward peak. The blue curve is our polarization curve reflected about 90° and modified for the finite range of symmetric charge transfer. The cyan points are from Vestal, Blakely, and Futrell[11].

Figure 8 shows elastic differential cross section versus scattering angle in center-of-mass for Ar^+ by Ar at 10 eV relative energy. The almost hidden purple curve is our construction based on reflection of the polarization scattering. The blue curve is our polarization curve reflected about 90° and modified for the finite range of symmetric charge transfer. The dark blue points are from Aberth and Lorents[10], while the cyan points are from Vestal, Blakely, and Futrell[11].

IX. $KR^+ + KR$

X. $XE^+ + XE$

XI. DISCUSSION

The polarization approximation used here for collisions between ions and their parent atoms also works reasonably well for ions with foreign atoms. See slide 18 in the file Ion-AtomGEC01.ppt for plots at low and moderate energies for the Na+ + Xe case.

Note that all of our suggested differential cross sections need to be smoothed using a function representing diffraction effects. This important at angle near zero and 180 degrees. See Massey and Mohr for a discussion of refractive effects and polarization scattering in the near-forward direction.

I need to look at other non-symmetric ion-molecule cases and the consider whether there are useful similar approximations for neutral-neutral differential scattering cross sections.

Acknowledgments

I thank A. Gallagher, C. H. Greene, and L. C. Pitchford for their helpful comments. This work was supported in part by JILA and by the National Institute of Standards and Technology.

APPENDIX A: SOME THOUGHTS ON SYMMETRIC CHARGE TRANSFER

THE FOLLOWING IS SLIGHTLY MODIFIED FROM NOTE ENTITLED: The comparison of experimental and theoretical symmetric charge transfer cross sections. A. V. Phelps, April 10, 2003

I have always thought of symmetric charge transfer as being that aspect of the differential scattering cross section that shows as a peak in the backward direction at high energies. This picture is the result of having been brought up on the model of symmetric charge transfer as the result of nearly straight line particle trajectories appropriate to relatively high collision energies, e.g., Holstein, J. Phys. Chem. 56, 832 (1952). However, this picture fails as the elastic differential scattering cross section becomes more isotropic at low collision energies.

Also, when looked at on a fine enough angle scale, the backward peak is generally lower than the forward peak and actually can be a dip (see 7 below) at 180° in center of mass.

It is important to note that the usual quantum mechanical expression for the symmetric charge transfer cross section is obtained by extending the picture appropriate to high energies to all energies. Thus, it is assumed that at high energies the forward and backward components of the scattering function do not interfere and can be evaluated separately. The backward component is identified as giving the charge transfer cross section. The resultant expression in then used under all conditions, e.g., even when the detailed calculations show strong interference effects at all angles. Many authors use this formula. Papers like Sinha, Lin, and Bardsley, J. Phys. B 12, 1613 (1979) and Krstic and Schulz (see below) are faintly critical of the formula, but do not say it is wrong. Thus, quantum mechanics texts give us a potentially questionably quantity to be compared with experiment.

Recently, it dawned on me that the symmetric charge transfer cross section results from quantum mechanics can be more accurately compared with experiment at most (all?) energies by measurement or calculation of the integrated scattering into the backward half sphere as used originally(?) by Hinds and Novick[**?**]. This empirical correlation can be seen to predict the right relation between the diffusion cross section and the charge transfer cross section for isotropic scattering, as for very low energies, and for backward scattering, as at high energies. In both of these cases the half-sphere, charge transfer cross section is easily shown to be half the momentum transfer or diffusion cross section.

Some points to consider are:

1)This change in the picture of symmetric charge transfer from a backward peak to the backward half sphere allows one "understand" the 2:1 cross section ratio found in several recent quantum mechanical calculations:

a) For the scattering of H+ by H at 0.1 eV, Fig. 8 of Krstic and Schulz, J. Phys. B 32, 3485 (1999) shows that it is essentially impossible to assign a backward scattering component to the elastic cross section. Yet Krstic and Schulz show, see Fig. 5, that the symmetric charge transfer cross section has its maximum values near 0.1 eV and is very nearly half the diffusion cross section at all energies.

b) Cote and Dalgarno, Phys. Rev. A 62, 012709 (2000) show that the theoretical charge transfer cross section for Na+ + Na is almost exactly half the diffusion (momentum transfer) cross section from 1E-15eV to 10 eV. The departures from 2:1 near 1E-5 eV may be the

result of interference effects. At very low energies the scattering is s-wave and the 2:1 ratio is expected.

2) The determination of symmetric charge transfer cross sections from measurements of scattering into the backward half-sphere was used by Hinds and Novick, J. Phys. B 11, 2201 (1978). These authors used a retarding grid set at one quarter of the beam energy to reject ions that have less than half their initial velocity in the beam direction after a collision. These authors claim that their measured cross section is equal to the charge transfer cross section to within a few percent, but do not give details. I think that there is another reference using this approach, but I have misplaced it.

3) Helm, J. Phys. B 10, 3683 (1977) takes the symmetric charge exchange cross section to be half the diffusion (momentum transfer) cross section determined from mobility measurements at all energies. So far, I have not found his argument for doing this at low energies. I question its validity.

4) As far as Monte Carlo calculations of ion transport are concerned, the definition of symmetric charge transfer as scattering into the back half-sphere results in a great deal of uncertainty as to what to assume for the differential cross section. The importance of this uncertainty is significantly reduced by the conclusion of Piscitelli and Pitchford (private communication) that the calculated mobilities of Ne+ in Ne and Xe+ in Xe are independent of whether one uses an isotropic elastic differential cross section or a two component (backward and isotropic) elastic differential scattering cross section with the same diffusion cross section.

5) A potentially significant loss to the simplicity of some ion transport models from this definition of symmetric charge transfer is breakdown of the idea that zero energy ions are produced by the collision with a "cold", parent gas atom. The idea is particularly useful at "high" energies because of the detailed behavior of the differential cross section within the backward half sphere.

6) The definition of the experimental symmetric charge transfer cross section as the integrated scattering in the backward half sphere considerably simplifies the interpretation of many beam measurements that make use of the collection of slow ions using a transverse electric field. This is because the details of the angular distribution of product ions is unimportant provided the ions are concentrated in the backward and forward directions in CM.

7) A point that is related to the above is that for the case of symmetrical ion scattering, the differential cross section should not be symmetrical about $90^c ir$ CM and that there should be a minimum in the differential cross section at 180° CM. Using classical trajectories, these effects are the result of impact parameters for which the distance of closest approach is outside the range of effective charge transfer and the corresponding scattering angle is too small for charge transfer to be effective. The result is a peak in the forward scattering at small angles that is not reflected about 90° and a corresponding deficiency of scattered particles at 180° CM. Calculations show that this structure is often not obscured by ion diffraction effects. These structures in the differential cross section can be seen in the theoretical results of Krstic and Schulz for H+ + H for 0.1 and 1 eV (Fig. 8). In the case of He+ + He, this effect shows as a lower scattering peak in the backward direction than in the forward direction - Sinha et al (1979).

8) Sinha et al (1979) point out that the "formulation of transport theory does not require the definition of a cross section for charge transfer".

---

[1] Nanbu and Kitatani 95 J. Phys. D 28, 324

[2] McDaniel E W, Mitchell, and Rudd, 1993 *Atomic Collisions: Heavy Particle Collisions* (Wiley, New York), p. 91.

[3] McDaniel E W 1964 *Collisions Processes in Gas Discharges* (Wiley, New York), p. ??.

[4] A. V. Phelps $ftp://jila.colorado.edu/collision\_data/readme.txt$ (unpublished).

[5] This statement follows from the fact that in symmetric charge transfer collisions there is no change in the sum of the internal energies of the incident particle compared to the sum of the energies of the identical product particles.

[6] Holstein T 1948 Phys Rev. ???????.

[7] Phelps A V 1994 J. Appl. Phys. ?????????.

[8] Cote and Dalgarno 200? Phys. Rev. A ?????????.

[9] Sinha, Lin, and Bardsley, J. Phys. B 12, 1613 (1979)

[10] Aberth and Lorents (1966)

[11] Vestal, Blakely, and Futrell (1978)

[12] Krstic and D. R. Shultz (1999).

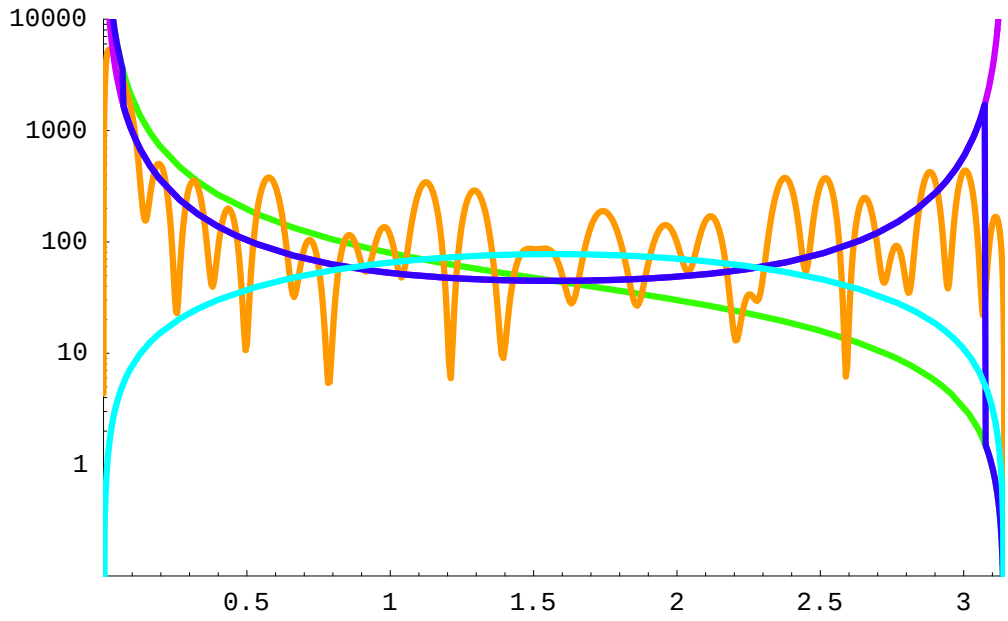

FIG. 1: Elastic differential cross section in a_0^2/sr versus scattering angle in $^\circ$ in center-of-mass for H^+ by H at 0.1 eV relative energy. The solid curves are from Kristic and Schulz. [12] Note absence of a backward peak as expected for "classical" symmetric charge transfer. The green curve is the polarization curve without taking symmetric charge transfer into account. The orange curve a constant differential cross section on this type of plot. The purple curve is our construction based on reflection of the polarization scattering. The blue curve is our polarization curve modified for the finite range of symmetric charge transfer.

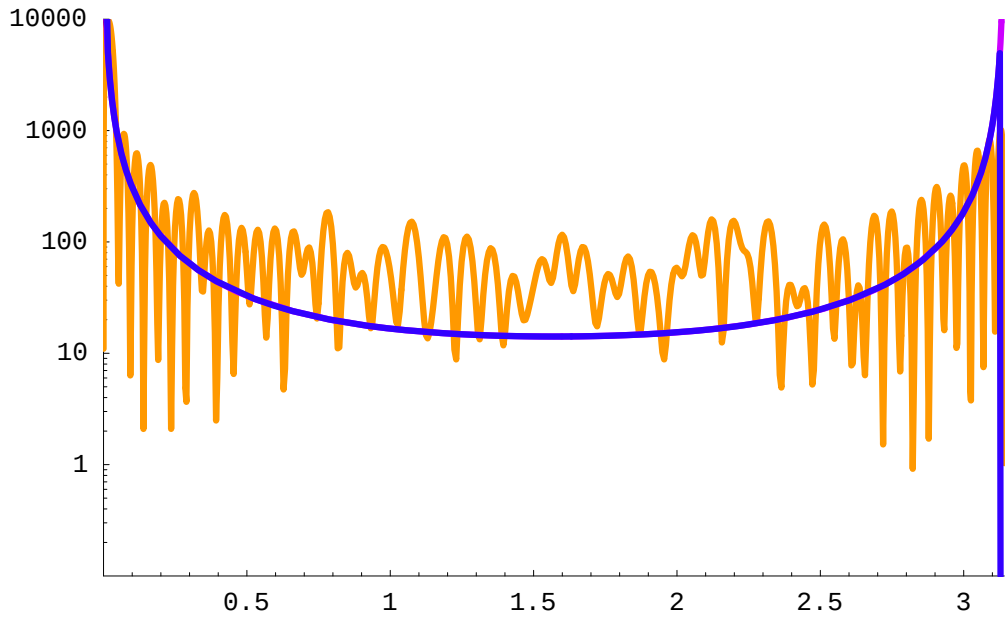

FIG. 2: Elastic differential cross section (a_0^2/sr) versus scattering angle (°) in center-of-mass for H^+ by H at 1 eV relative energy. The solid curves are from Kristic and Schulz. [12] Note absence of a backward peak. The almost hidden purple curve is our construction based on reflection of the polarization scattering. The blue curve is our polarization curve modified for the finite range of symmetric charge transfer.

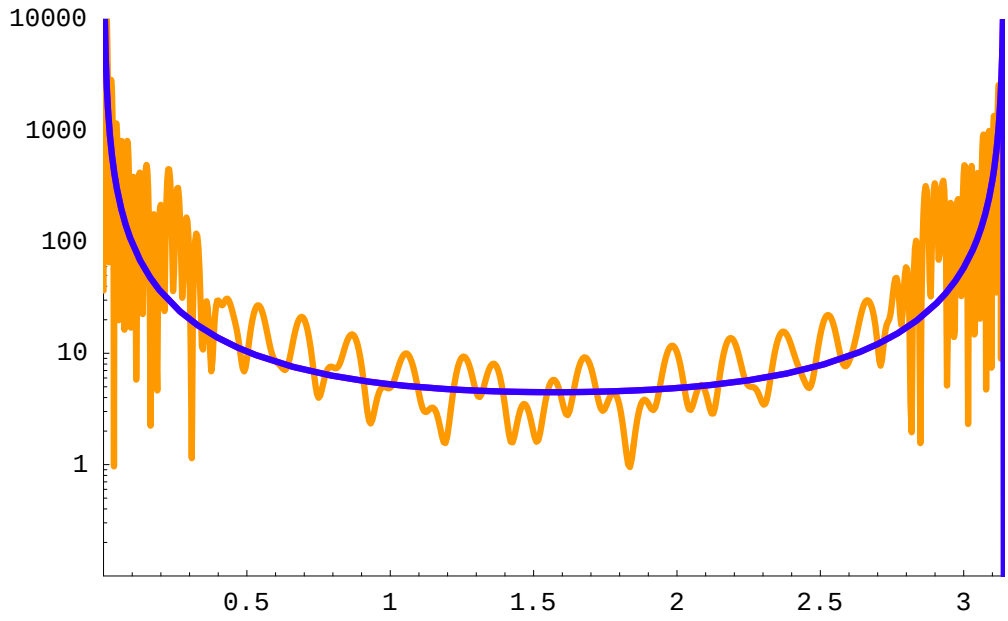

FIG. 3: Elastic differential cross section (a_0^2/sr) versus scattering angle (°) in center-of-mass for H^+ by H at 10 eV relative energy. The solid curves are from Kristic and Schulz. [12] The almost hidden purple curve is our construction based on reflection of the polarization scattering. The blue curve is our polarization curve modified for the finite range of symmetric charge transfer.

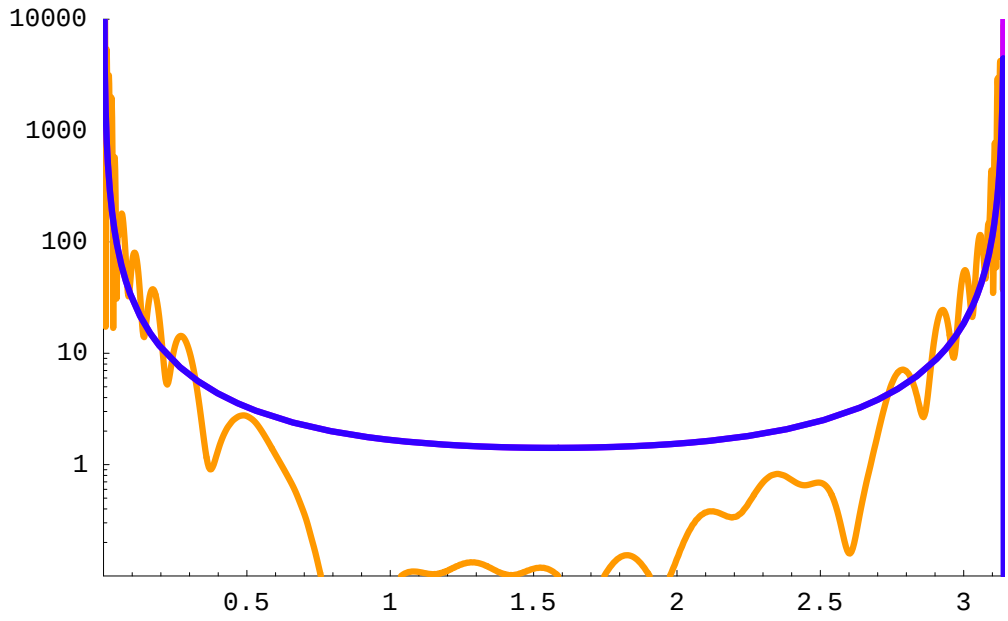

FIG. 4: Elastic differential cross section (a_0^2/sr) versus scattering angle in center-of-mass (°) for H^+ by H at 100 eV relative energy. The solid curves are from Kristic and Schulz. [12] The almost hidden purple curve is our construction based on reflection of the polarization scattering. The blue curve is our polarization curve modified for the finite range of symmetric charge transfer.

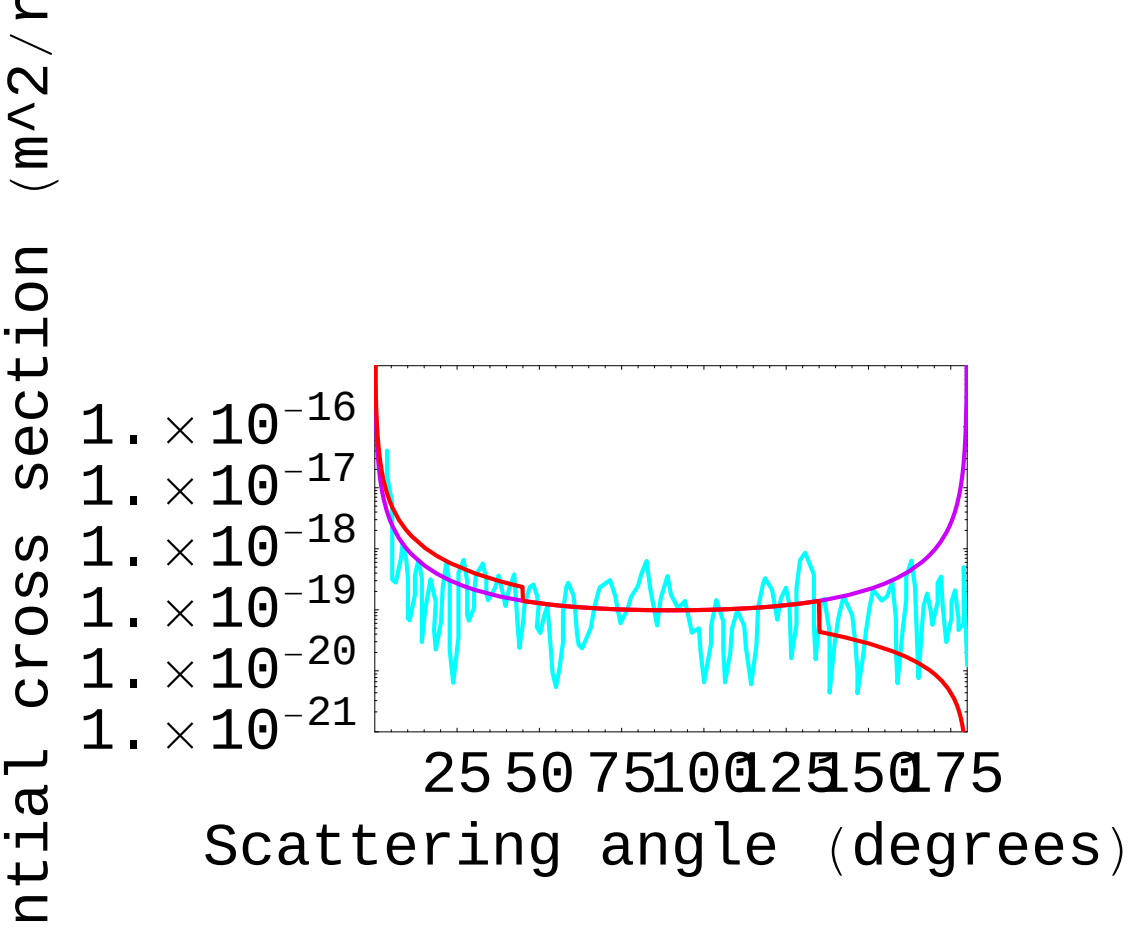

FIG. 5: Elastic differential cross section (m^2/sr) versus scattering angle in center-of-mass (°) for He^+ by He at 0.05 eV relative energy. The cyan curve are from Kristic and Schulz. [12] Note absence of a backward peak. The purple curve is our construction from polarization scattering assuming symmetrical charge transfer means reflection about 90 deg. The red curve is our modification that roughly accounts for the finite range of symmetric charge transfer.

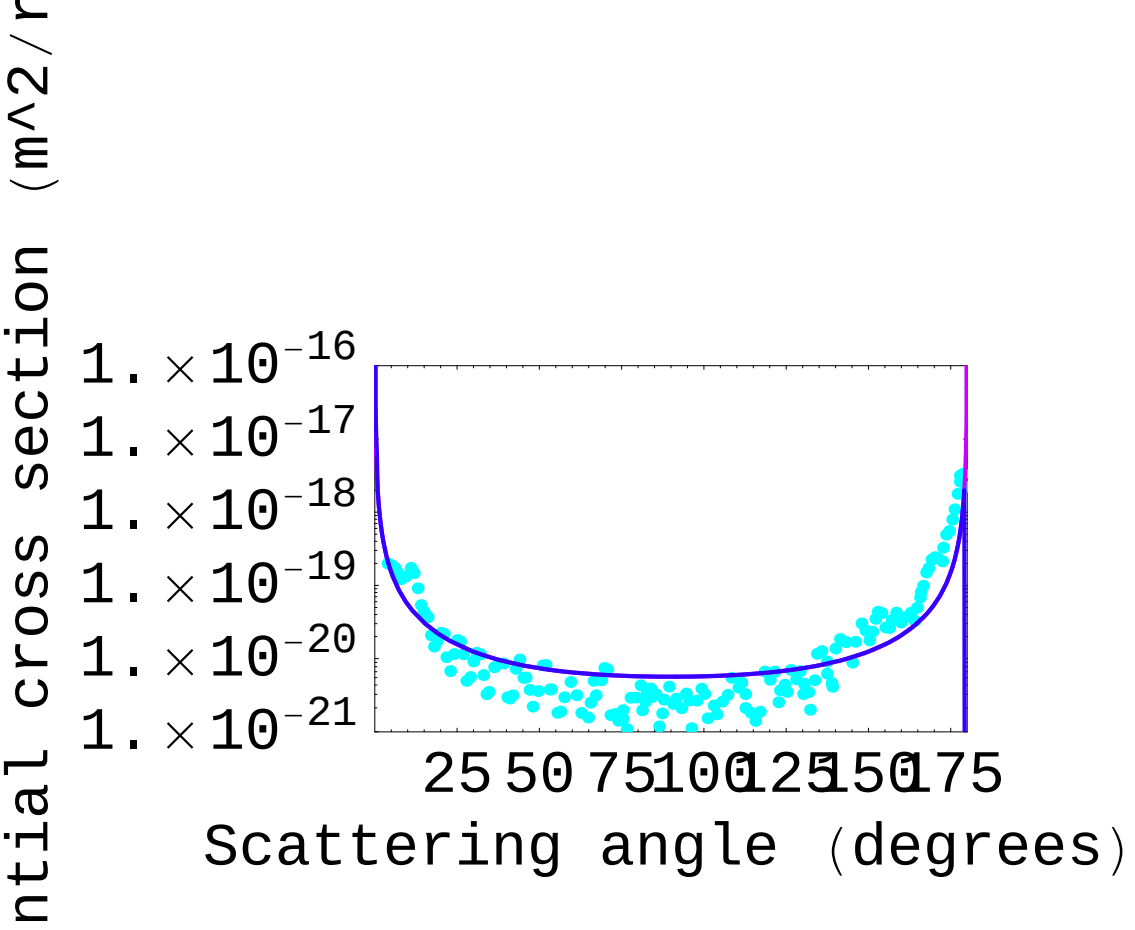

FIG. 6: Elastic differential cross section (m^2/sr) versus scattering angle (°) in center-of-mass for He^+ by He at 15 eV relative energy. The solid curves are from Kristic and Schulz. [12] The blue curve is our polarization curve modified for the finite range of symmetric charge transfer. The cyan points are from Vestal, Blakely, and Futrell [11].

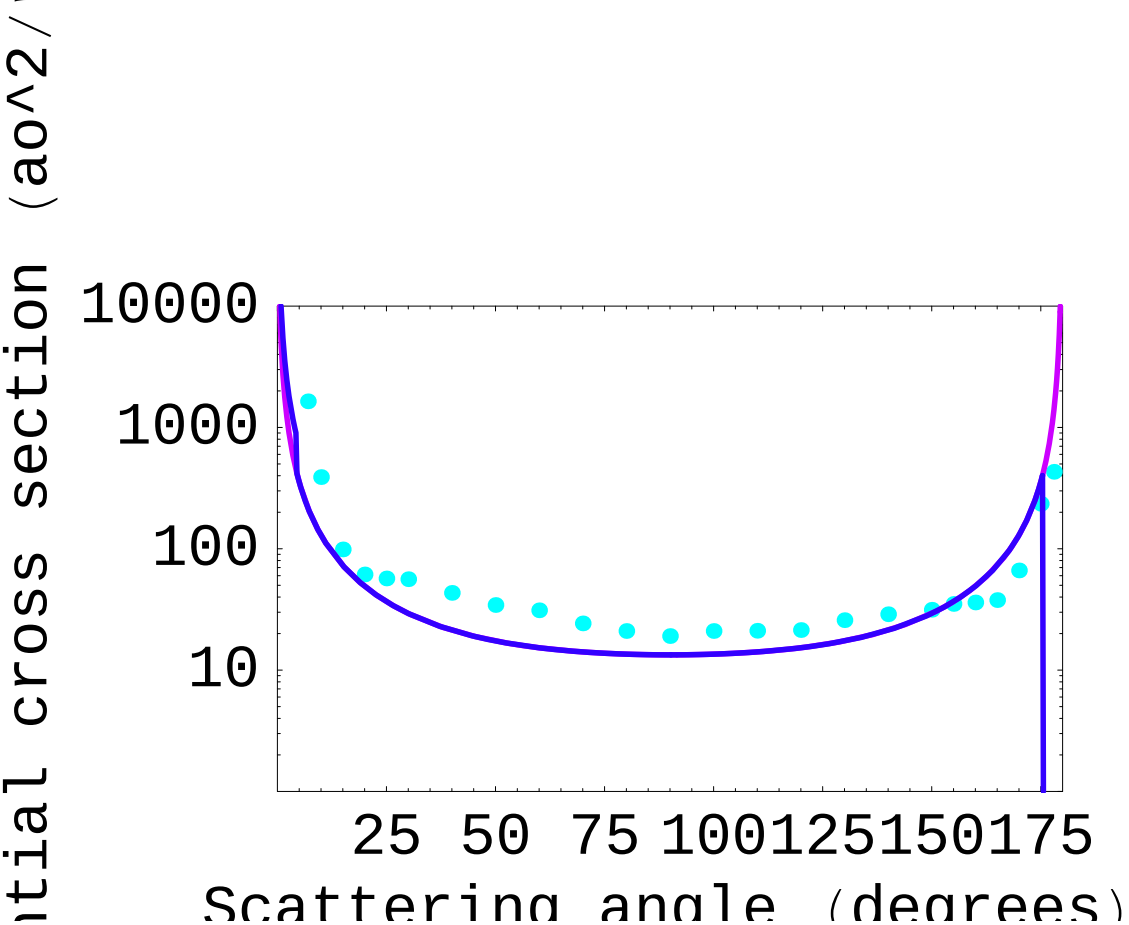

FIG. 7: Elastic differential cross section (a_0^2/sr) versus scattering angle in center-of-mass (°) for Ar^+ by Ar at 2.76 eV relative energy. Note the reduction in the backward peak relative to the forward peak. The blue curve is our polarization curve modified for the finite range of symmetric charge transfer. The cyan points are from Vestal, Blakely, and Futrell[11].

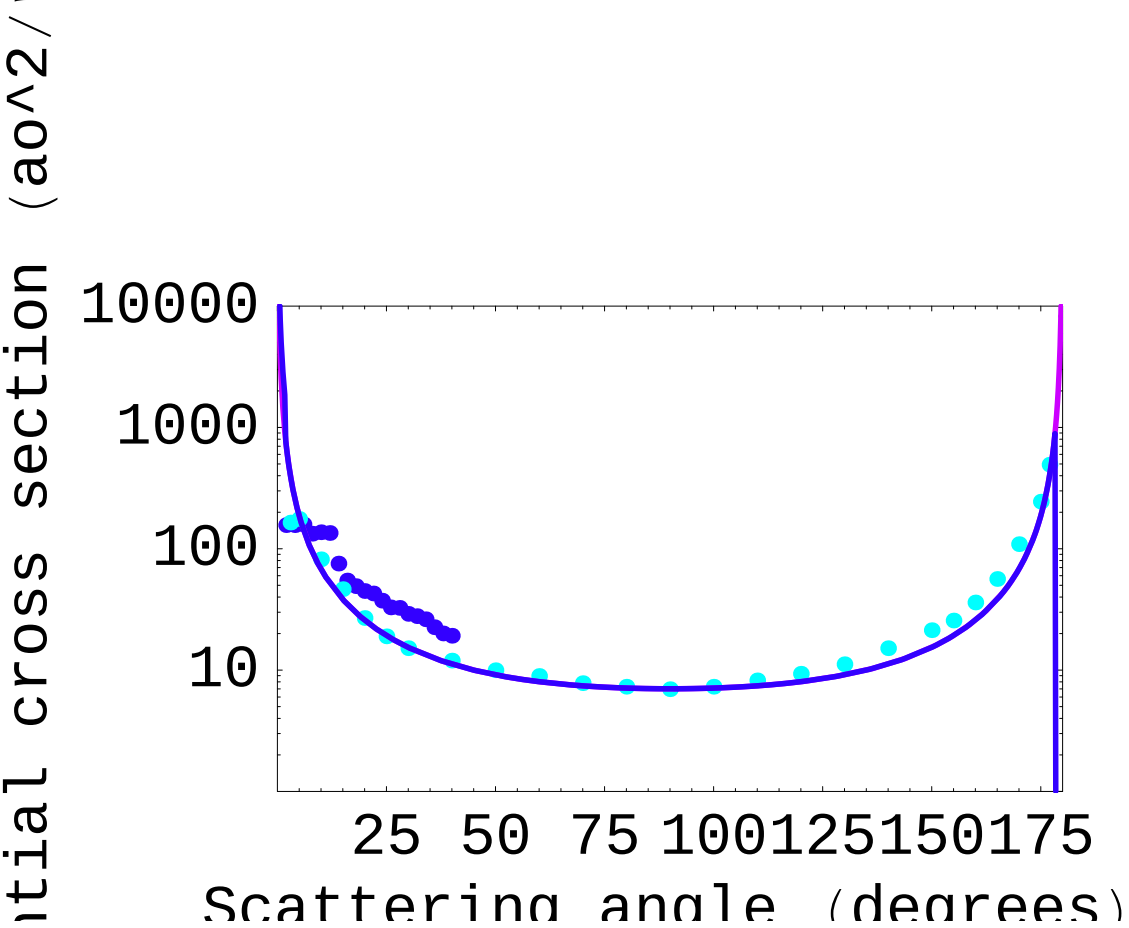

FIG. 8: Elastic differential cross section (a_0^2/sr) versus scattering angle (°) in center-of-mass for Ar^+ by Ar at 10 eV relative energy. The almost hidden purple curve is our construction based on reflection of the polarization scattering. The blue curve is our polarization curve modified for the finite range of symmetric charge transfer. The dark blue points are from Aberth and Lorents[10], while the cyan points are from Vestal, Blakely, and Futrell[11].